IOP Conf. Series: Journal of Physics: Conf. Series **1023** (2018) 012010 doi:10.1088/1742-6596/1023/1/012010

From *ab initio* structure predictions to reaction calculations via EFT

P. Capel[1,2,3], V. Durant[2,3], L. Huth[2,3], H.-W. Hammer[2,3], D. R. Phillips[4], and A. Schwenk[2,3,5]

E-mail: pierre.capel@ulb.ac.be,
durant@theorie.ikp.physik.tu-darmstadt.de,
lukashuth@theorie.ikp.physik.tu-darmstadt.de,
hans-werner.hammer@physik.tu-darmstadt.de,
phillid1@ohio.edu,
schwenk@physik.tu-darmstadt.de

[1]Physique Nucléaire et Physique Quantique (CP 229), Université libre de Bruxelles (ULB), B-1050 Brussels
[2]Institut für Kernphysik, Technische Universität Darmstadt, 64289 Darmstadt, Germany
[3]ExtreMe Matter Institute EMMI, GSI Helmholtzzentrum für Schwerionenforschung GmbH, 64291 Darmstadt, Germany
[4]Institute of Nuclear and Particle Physics and Department of Physics and Astronomy, Ohio University, Athens, OH 45701,USA
[5]Max-Planck-Institut für Kernphysik, Saupfercheckweg 1, 69117 Heidelberg, Germany

Abstract. We study how EFT can improve the description of reactions used to study the structure of exotic nuclei. Using Halo EFT helps constraining the potential that simulates the interaction between the projectile constituents. It enables us to include *ab initio* results within the reaction model and to clearly identify the nuclear properties probed by the reaction. New local chiral EFT nucleon-nucleon interactions can also be used to derive nucleus-nucleus optical potentials from first principles, which can provide reliable inputs in reaction modelling.

1. Introduction

Halo nuclei have been discovered thanks to the development of radioactive-ion beams in the mid-80s [1]. Compared to their isobars, they exhibit very large reaction cross sections on light targets that have been interpreted as the sign of a matter radius larger than the $A^{1/3}$ behaviour observed for stable and many other nuclei. This unusual size is qualitatively understood as resulting from a strongly clusterised structure: halo nuclei are seen as a compact core to which one or two neutrons are loosely bound. Thanks to this loose binding the valence neutrons exhibit a high probability of presence at a large distance from the other nucleons, forming a diffuse halo around the core. This exotic nuclear structure is encountered at the limit of stability, where the binding energy for one or two neutrons becomes very small. The nucleus ^{11}Be is an archetypical one-neutron halo nucleus, while ^{11}Li exhibits a two-neutron halo. Due to their exotic structure, halo nuclei are a challenge for nuclear-structure models. Very recently, Calci *et al.* have been able to compute ^{11}Be within a No-Core Shell Model with continuum calculation (NCSMC) [2], managing to describe the halo structure, the ^{10}Be-n continuum, and the well-known shell inversion between the $1/2^+$ ground state and the $1/2^-$ bound excited state.

Being located at the limit of stability, halo nuclei exhibit very short lifetimes, which makes it difficult to employ the usual spectroscopic techniques to study their structure. Therefore, they are usually studied indirectly through reactions like transfer (see the contribution of Yang in these proceedings [3]) or breakup [4]. In the latter reaction, the halo dissociates from the core during the collision with a target. To get valuable information from such measurements, an accurate reaction model coupled to a realistic description of the projectile and reliable inputs for the models are needed. In this contribution, we explore how effective field theory (EFT) can help us build a realistic few-body description of ^{11}Be from the *ab initio* calculation of Calci *et al.* [2] and how it could help us derive the optical potentials needed as inputs for the reaction model from first principles. The former task is performed within the EFT description of halo nuclei [5, 6]; for the latter, we test the double-folding of a local chiral EFT nucleon-nucleon interaction with the density of the projectile and the target [7].

After a quick presentation of the reaction model we consider in this study, we present in Sec. 3 how the *ab initio* results are described within the Halo EFT. In Sec. 4, we summarise the first results obtained using a double-folding procedure to derive optical potentials from first principles. Finally, we conclude in Sec. 5

2. Reaction model

We consider reactions in which the one-neutron halo nucleus ^{11}Be interacts with a target. The simplest way to describe such collisions is to consider a two-body model of the projectile, hence seen as an inert ^{10}Be core in its 0^+ ground state to which a neutron is loosely bound [8]. Such structure is described by the Hamiltonian

$$H_0 = T_r + V_{\mathrm{cn}}(\boldsymbol{r}), \tag{1}$$

where the effective potential V_{cn} simulates the interaction between the ^{10}Be core c and the valence neutron n. The particulars about this interaction will be detailed in Sec. 3.

The internal structure of the target T is neglected and its interaction with the projectile constituents is described by optical potentials V_{cT} and $V_{\mathrm{n}T}$. So far these potentials are taken from the literature, where they have been adjusted to reproduce elastic-scattering data. In Sec. 4, we will explore how they could be derived from first principles using a double-folding procedure.

Within this model, the study of the reaction reduces to solving the following three-body Schrödinger equation

$$\left[T_R + H_0 + V_{cT} + V_{\mathrm{n}T}\right] \Psi(\boldsymbol{r}, \boldsymbol{R}) = E_T \, \Psi(\boldsymbol{r}, \boldsymbol{R}) \tag{2}$$

with the initial condition that the incoming projectile is initially in its ground state ϕ_0:

$$\Psi(\boldsymbol{r}, \boldsymbol{R}) \underset{Z \to -\infty}{\longrightarrow} e^{iKZ} \phi_0(\boldsymbol{r}). \tag{3}$$

Various techniques exist to solve this problem, see Ref. [8] for a recent review. We will use the dynamical eikonal approximation (DEA) [9, 10], which is very efficient and precise at the beam energies considered here [11].

3. Including Halo EFT within reaction models

3.1. EFT description of ^{11}Be

Usually, the potential that simulates the c-n interaction within reaction models exhibits a Woods-Saxon form factor. The depth of that potential is then adjusted to reproduce the basic properties of the projectile, like its binding energy and the quantum numbers of its ground state. We suggest

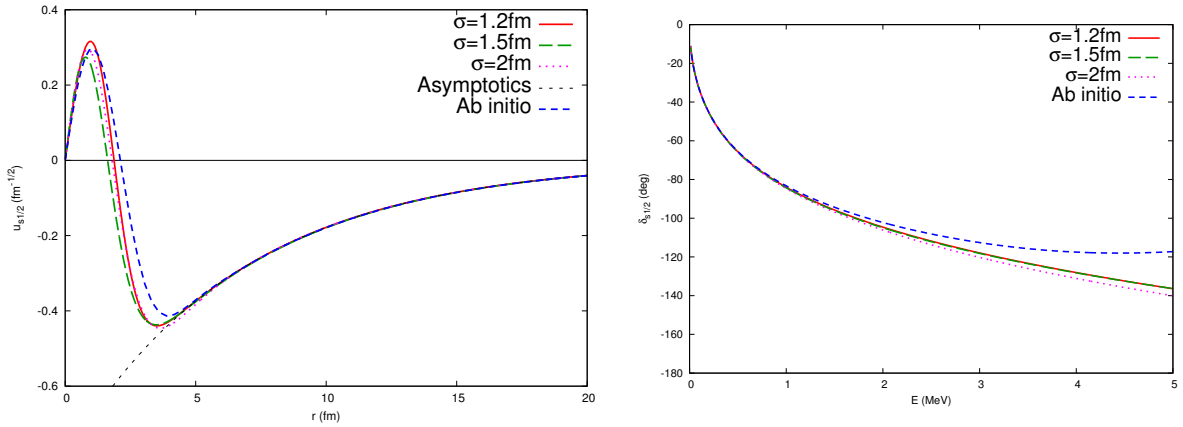

Figure 1. Left: $1s_{1/2}$ reduced radial wave function describing the $1/2^+$ ground state of ^{11}Be. Right: $s_{1/2}$ phase shift. Calculations performed within the Halo EFT description of ^{11}Be with different Gaussian width σ are confronted to the *ab initio* predictions [2].

to replace this phenomenological interaction by an effective interaction based on Halo EFT [5]. We use a Gaussian shape which, at next-to-leading order (NLO), can be taken to be [6]

$$V_{lj}(r) = V_{lj}^0 \; e^{-\frac{r^2}{2\sigma^2}} + V_{lj}^2 \; r^2 e^{-\frac{r^2}{2\sigma^2}}. \tag{4}$$

In each partial wave of orbital angular momentum l and total spin j, such a form gives us two parameters that can be adjusted to reproduce the energy of the projectile states and their asymptotic normalisation constant (ANC), for bound states, or their width, for resonant states. The low-energy spectrum of ^{11}Be is well known, however the ANC of its two bound states have not been directly measured. To help us in this task, we rely on the *ab initio* calculation of Calci *et al.* which is the most advanced calculation of ^{11}Be available so far [2].

The Gaussian width σ is a length scale that helps us evaluate the sensitivity of the reaction model to short-range physics. In the following, we consider $\sigma = 1.2$, 1.5, and 2 fm.

This two-body model of ^{11}Be assumes that its $1/2^+$ ground state corresponds to the single-particle state in which the valence neutron sits in the intruder $1s_{1/2}$ partial wave. The $1/2^-$ bound excited state corresponds to the regular $0p_{1/2}$ shell-model state. The reduced radial wave function is plotted in the left panel of Fig. 1 for the different Gaussian widths $\sigma = 1.2$ (red solid line), 1.5 (green dashed line), and 2 fm (magenta dotted line). These Halo EFT wave functions are compared to the *ab initio* result [2] (blue short-dashed line). All wave function exhibit the same asymptotic behaviour since our Gaussian potentials have been fitted to reproduce the binding energy and the ANC of the *ab initio* calculation. However, they significantly differ in the interior as expected from the difference in the short-range scale chosen for each potential.

The right panel of Fig. 1 displays the $s_{1/2}$ phase shift obtained by the three different Gaussian potentials. Since they have been adjusted to the same binding energy and ANC, they exhibit very similar phase shifts, especially at low energy, where their effective-range expansion is nearly identical [6]. These phase shifts compare very well with the *ab initio* prediction up to $E = 1$–1.5 MeV in the ^{10}Be-n continuum. Similar results are obtained in the $p_{1/2}$ partial wave. In the strict Halo EFT taken at NLO, the ^{10}Be-n interaction is switched off in all other partial waves, either because there is no low-energy state that generates a significant phase shift, or because their orbital angular momentum is too high.

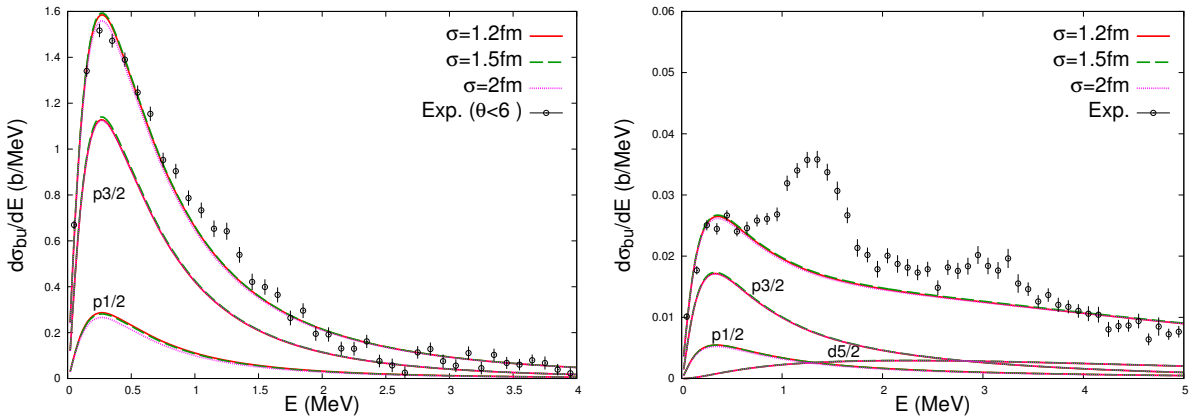

Figure 2. Energy distributions for the breakup of ^{11}Be on Pb at 69AMeV (left) and on C at 67AMeV (right). The data are from Ref. [4].

3.2. Breakup of ^{11}Be

Starting from the effective description of ^{11}Be derived in the previous section, we perform breakup calculations within the DEA using the numerical condition and inputs (viz. optical potentials) of Ref. [10]. We consider the experimental conditions of the RIKEN experiment [4]: a Pb target at 69AMeV and a C target at 67AMeV. The corresponding breakup cross section are plotted in Fig. 2 as a function of the ^{10}Be-n relative energy E after dissociation [6]. The contributions of the dominant partial waves are depicted as well.

It is interesting to note that in both cases, the computed cross sections are nearly identical for all three different descriptions of ^{11}Be. This confirms that—at least in the non-resonant continuum—breakup is a peripheral process, in the sense that it probes only the tail of the wave function [12]. Accordingly the three different descriptions, which produce identical ANCs for the ground state, lead to identical cross sections. Interestingly, this is true even on light targets, for which the reaction is dominated by the short-range nuclear interaction.

As expected from a collision on a heavy target, the breakup on Pb (Fig. 2 left) is mostly Coulombian. Therefore, the major partial waves populated in the continuum are the p waves. In this case, the agreement with the RIKEN data are excellent, without any fitting parameter. This confirms the value of the ground-state ANC predicted by the *ab initio* calculation.

The collision on C (Fig. 2 right) populates, in addition to the p waves, a significant amount of the d-wave continuum. In this case, the agreement with the data is less good. Although it produces the right order of magnitude and the general trends of the data, our calculations clearly miss the low-energy peak that corresponds to the $5/2^+$ state in the ^{10}Be-n continuum. That state is usually described as a single-particle $d_{5/2}$ resonance [13]. Unfortunately, adding that state in an extension of our Halo EFT description of ^{11}Be does not fully solve the problem [6]. This suggests that some significant degrees of freedom are missing in order to correctly describe that state and its influence on the reaction calculation. Within the Halo EFT expansion scheme, the first degree of freedom that has been overlooked in our model would most certainly be the first 2^+ excited state of the ^{10}Be core. Adding this state in an extension of the present model would most likely improve our comparison with the data. This is one of our goals for the future.

4. Deriving optical potential from first-principle chiral EFT NN interactions

4.1. Double-folding procedure

The core of halo nuclei is usually itself radioactive; it is therefore difficult to find the proper optical potential to describe its interaction with the target. To see if it can be derived from first principles, we study the development of an optical potential from chiral EFT nucleon-nucleon (NN) interactions using a double-folding procedure. To perform these calculations, we take advantage of the recent development of local chiral EFT NN interactions [14, 15].

The potential is built at the Hartree-Fock level, including both the direct and exchange terms [16]

$$V_F(\boldsymbol{r}, E_{\rm cm}) = V_{\rm D}(\boldsymbol{r}) + V_{\rm Ex}(\boldsymbol{r}, E_{\rm cm}) \tag{5}$$

The former is calculated by integrating the NN interaction over the neutron (n) and proton (p) density distributions $\rho_1^{\rm n,p}$ and $\rho_2^{\rm n,p}$ of the colliding nuclei,

$$V_{\rm D}(\boldsymbol{R}) = \sum_{i,j={\rm n,p}} \int\int \rho_1^i(\boldsymbol{r}_1)\, v_{\rm D}^{ij}(\boldsymbol{S})\, \rho_2^j(\boldsymbol{r}_2)\, d^3\boldsymbol{r}_1 d^3\boldsymbol{r}_2\,, \tag{6}$$

where $\boldsymbol{R}$ is the relative coordinate between the centre of mass of the nuclei, $\boldsymbol{r}_1$ and $\boldsymbol{r}_2$ are the coordinates from the centre of mass of each nucleus, $\boldsymbol{S} = \boldsymbol{R} - \boldsymbol{r}_1 + \boldsymbol{r}_2$, and the sum i, j is over neutrons and protons with their respective densities. The exchange term reads

$$V_{\rm Ex}(\boldsymbol{R}, E_{\rm cm}) = \sum_{i,j={\rm n,p}} \int\int \rho_1^i(\boldsymbol{r}_1, \boldsymbol{r}_1 + \boldsymbol{S})\, v_{\rm Ex}^{ij}(\boldsymbol{S}) \rho_2^j(\boldsymbol{r}_2, \boldsymbol{r}_2 - \boldsymbol{S}) \exp\left[\frac{i\boldsymbol{K}(\boldsymbol{R})\cdot\boldsymbol{S}}{\mu/m_{\rm N}}\right] d^3\boldsymbol{r}_1 d^3\boldsymbol{r}_2\,, \tag{7}$$

where $\mu = m_{\rm N} A_1 A_2/(A_1 + A_2)$ is the reduced mass of the colliding nuclei (with $m_{\rm N}$ the nucleon mass) and the integral is over the density matrices $\rho^i(\boldsymbol{R}, \boldsymbol{R} \pm \boldsymbol{S})$ of the nuclei. The momentum for the NN relative motion $\boldsymbol{K}$ is related to $E_{\rm cm}$ and the double-folding potential [16, 7].

Following this method, we calculate double-folding potentials at LO, NLO and N^{2}LO, using different cutoffs R_0 [7]. Examples of the potentials we obtain are presented in the left panel of Fig. 3. We observe a systematic order-by-order behaviour expected in EFT. Moreover, we see that the potential exhibits a rather small dependence on the cutoff, indicating that it is not very sensitive to the short-range details of the NN interaction.

In addition to the real part provided by Eq. (5), optical potentials also include an imaginary part that simulates the absorption from the elastic channel due to other open channels, like inelastic scattering or transfer. In this first attempt, we follow the São Paulo group and assume the imaginary part to be proportional to the real part obtained by double folding [18]

$$U_F(r) = (1 + i\, N_W)\, V_F(r), \qquad \text{with } N_W = 0.6\text{–}0.8. \tag{8}$$

4.2. ^{16}O-^{16}O *scattering and fusion*

To evaluate the validity of our potentials, we perform calculations for ^{16}O-^{16}O elastic scattering at different energies and compare them to data [7]. This is illustrated in the right panel of Fig. 3, where the ratio of the elastic-scattering cross section is presented as a ratio to the Mott cross section at $E_{\rm lab} = 350$ MeV. Interestingly, we observe the very same systematic order-by-order behaviour expected in the EFT as in the double-folding calculation (see the left panel of Fig. 3). We also note that the sensitivity to the cutoff R_0 is rather small and becomes noticeable only at sufficiently large angles ($\theta > 20°$–$25°$). The agreement with the data is quite good, given that there is no parameter adjusted to fit the data. However, there remains some uncertainty to the choice of the scaling of the imaginary part N_W [7].

IOP Conf. Series: Journal of Physics: Conf. Series **1023** (2018) 012010 doi:10.1088/1742-6596/1023/1/012010

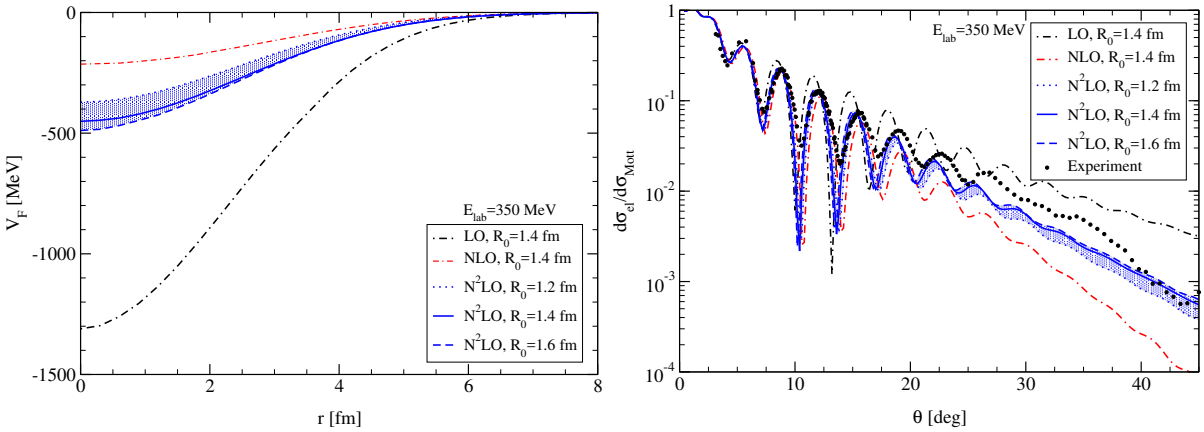

Figure 3. ^{16}O-^{16}O elastic scattering at $E_{\rm lab} = 350$ MeV. Left: double-folding potential built from local chiral EFT NN interactions at LO, NLO and N^{2}LO [7]. Right: elastic-scattering cross section as a ratio to Mott cross section obtained with these potentials. Data are from Ref. [17].

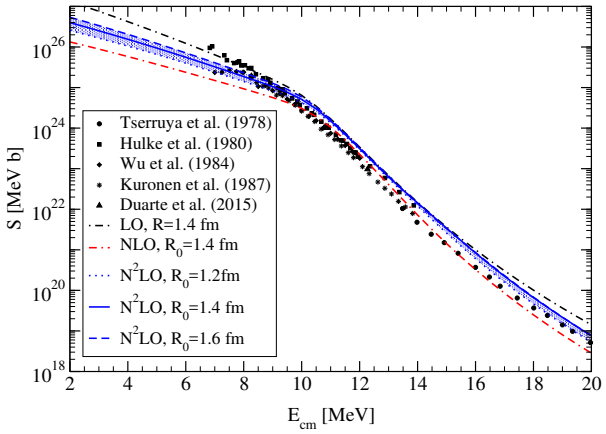

Figure 4. Astrophysical S factor for the ^{16}O-^{16}O fusion as a function of the centre-of-mass energy $E_{\rm cm}$ [7]. The data are from Refs. [19, 20, 21, 22, 23].

We can also check the reliability of our double-folding potential by computing the astrophysical S factor for ^{16}O-^{16}O fusion, which has been measured at various energies [19, 20, 21, 22, 23]. The results of this test are displayed in Fig. 4. As in the previous case, we observe the expected EFT order-by-order behaviour and note once more that the sensitivity of this observable to the details of the NN interaction remains small [7]. The agreement with the data are rather good, given that no parameter has been adjusted to fit the data.

5. Conclusion

In this work, we study the possibilities offered by EFT to improve the modelling of reactions involving halo nuclei. First, Halo EFT [5] provides an efficient tool to include the relevant degrees of freedom of the projectile nuclear structure within the few-body model of reactions. It also enables us to account for the outputs of *ab initio* nuclear-structure models within reaction calculations. The excellent agreement we have obtained for non-resonant breakup calculations using these outputs confirm their validity. The systematic study of these reactions with an EFT

description of the projectile also shows which degrees of freedom are required in order to properly describe the projectile and obtain theoretical cross sections in agreement with experiments. In particular, our analysis shows that the ^{10}Be core excitation plays a significant role in the resonant breakup of ^{11}Be in the collision on a C target.

Second, we have shown how the recently derived local chiral EFT NN interactions [14, 15] can be used to build the nucleus-nucleus optical potentials required in the modelling of nuclear reactions. Using a double-folding technique, we have produced optical potentials that provide elastic-scattering cross sections and astrophysical S factors for fusion in good agreement with ^{16}O-^{16}O data [7]. These preliminary results are very encouraging. An important uncertainty remains about the choice of the imaginary part of the potential, and we plan to focus our future work in this direction.

These first attempts of combining EFT used in nuclear structure with an accurate few-body description of nuclear reactions are very promising. Our results show that it could lead to a significant improvement of the reaction modelling for exotic nuclei and, accordingly, to a better analysis of reaction measurements at radioactive-beam facilities.

Acknowledgments

This work was supported in part by the European Union's Horizon 2020 research and innovation programme under grant agreement No 654002 and from the European Research Council Grant No. 307986 STRONGINT, the GSI-TU Darmstadt cooperation. This research was also supported by the U.S. Department of Energy under grant DE-FG02-93ER40756, by the German Federal Ministry of Education and Research under contract 05P15RDFN1, and by the Deutsche Forschungsgemeinschaft within the Collaborative Research Center 1245 (SFB 1245).

References

[1] Tanihata I 1996 *J. Phys. G* **22** 157
[2] Calci A, Navrátil P, Roth R, Dohet-Eraly J, Quaglioni S and Hupin G 2016 *Phys. Rev. Lett.* **117** 242501
[3] Yang J and Capel P 2017 contribution to this workshop
[4] Fukuda N, Nakamura T, Aoi N, Imai N, Ishihara M, Kobayashi T, Iwasaki H, Kubo T, Mengoni A, Notani M, Otsu H, Sakurai H, Shimoura S, Teranishi T, Watanabe Y X and Yoneda K 2004 *Phys. Rev. C* **70** 054606
[5] Hammer H W, Ji C and Phillips D R 2017 *J. Phys. G* **44** 103002
[6] Capel P, Phillips D and Hammer H W 2017 in preparation
[7] Durant V, Capel P, Huth L, Balantekin A B and Schwenk A 2017 *ArXiv e-prints* (*Preprint* `1708.02527`)
[8] Baye D and Capel P 2012 *Clusters in Nuclei, Vol. 2* vol 848 ed Beck C (Heidelberg: Springer)
[9] Baye D, Capel P and Goldstein G 2005 *Phys. Rev. Lett.* **95** 082502
[10] Goldstein G, Baye D and Capel P 2006 *Phys. Rev. C* **73** 024602
[11] Capel P, Esbensen H and Nunes F M 2012 *Phys. Rev. C* **85** 044604
[12] Capel P and Nunes F M 2007 *Phys. Rev. C* **75** 054609
[13] Capel P, Goldstein G and Baye D 2004 *Phys. Rev. C* **70** 064605
[14] Gezerlis A, Tews I, Epelbaum E, Gandolfi S, Hebeler K, Nogga A and Schwenk A 2013 *Phys. Rev. Lett.* **111** 032501
[15] Huth L, Tews I, Lynn J E and Schwenk A 2017 *ArXiv e-prints* (*Preprint* `1708.03194`)
[16] Furumoto T, Horiuchi W, Takashina M, Yamamoto Y and Sakuragi Y 2012 *Phys. Rev. C* **85** 044607
[17] Bohlen H G, Stiliaris E, Gebauer B, von Oertzen W, Wilpert M, Wilpert T, Ostrowski A, Khoa D T, Demyanova A S and Ogloblin A A 1993 *Z. Phys. A* **346** 189
[18] Pereira D, Lubian J, Oliveira J R B, de Sousa D P and Chamon L C 2009 *Phys. Lett. B* **670** 330
[19] Tserruya I, Eisen Y, Pelte D, Gavron A, Oeschler H, Berndt D and Harney H L 1978 *Phys. Rev. C* **18** 1688
[20] Hulke G, Rolfs C and Trautvetter H P 1980 *Z. Phys. A* **297** 161
[21] Wu S C and Barnes C 1984 *Nucl. Phys. A* **422** 373
[22] Kuronen A, Keinonen J and Tikkanen P 1987 *Phys. Rev. C* **35** 591
[23] Duarte J G, Gasques L R, Oliveira J R B, Zagatto V A B, Chamon L C, Medina N, Added N, Seale W A, Alcántara-Núñez J A, Rossi Jr E S *et al.* 2015 *J. Phys. G* **42** 065102